Polymer Chemistry

Accepted Manuscript

ROYAL SOCIETY OF CHEMISTRY

www.rsc.org/polymers

Cite this: DOI: 10.1039/c0xx00000x

www.rsc.org/xxxxxx

ARTICLE TYPE

Study on tunable AIE (AIEE) of boron ketoiminate-based conjugated polymers for live cell imaging†

Chunhui Dai,[a] Dongliang Yang,[b] Xiao Fu,[b] Qingmin Chen,[a] Chengjian Zhu,[a] Yixiang Cheng*[a] and Lianhui Wang*[b]

Received (in XXX, XXX) Xth XXXXXXXXX 20XX, Accepted Xth XXXXXXXXX 20XX
DOI: 10.1039/b000000x

ABSTRACT: In this study, four boron ketoiminate-based conjugated polymers **P1-P4** are designed and synthesized via Suzuki polymerization. The resulting polymers are weakly fluorescent in pure THF solutions, but become highly emissive when aggregated in THF/water mixtures or fabricated into conjugated polymer nanoparticles (CPNs), showing typical AIE (AIEE) behaviors. CPNs from **P1-P4** could be prepared by reprecipitation with the particle size ranging from 85 to 95 nm. Interestingly, the tuning of emission color of **P1-P4** nanoparticles (NPs) could be conveniently accomplished by varying substituent in the phenyl ring, which can be ascribed to donor-acceptor interaction between substituted phenyl ring and boron chelating ring. The DFT theoretical calculation of the polymer repeating units indicates that the band gaps of **P1-P4** can be tuned in the range 2.72–3.40 eV, suggesting that substituents in the polymer backbone have a great influence on their electronic structures and thus change AIE (AIEE) properties. Furthermore, all of the four CPNs with low cytotoxicity and high photostability could be further employed for HeLa cell imaging.

Received (in XXX, XXX) Xth XXXXXXXXX 20XX, Accepted Xth XXXXXXXXX 20XX
DOI: 10.1039/b000000x

Introduction

In recent years, luminescent organoboron polymers have drawn particular interest due to their superior properties as the advanced functional materials for optical and biological applications.[1] The incorporation of the boron atom into the conjugation system typically decreases the LUMO energy level of the polymers and thereby endows them with distinct optical and electric properties, such as excellent stability, extraordinary brightness in solution or aggregate state, long-wavelength fluorescence emission (even up to near-infrared (NIR) region), and the strong electron acceptability, and so on.[2] Significant efforts have been devoted to develop novel organoboron polymers with tunable optical properties and improve their performance for biomedical and optical application.[3] In our previous work, we have also reported some organoboron conjugated polymers, including chiral organoboron polymers, and BODIPY-based conjugated polymers with tunable NIR fluorescence emission, *etc*.[4]

It is well known that aggregation-induced emission (AIE) or aggregation-induced emission enhancement (AIEE) are interesting photophysical phenomenons. AIE (AIEE) luminogens are usually weakly emissive in solution, but can exhibit strong fluorescence in the aggregate state.[5] But most of luminogens would encounter aggregation-caused quenching (ACQ) effect, which limits their potential application for biological fluorescence probes. AIE-active materials have offered a powerful and versatile tool for bioprobes due to strong photoluminescence emission when their nanoaggregates disperse in aqueous solution. Recently, many AIE-active molecules have been developed and extensively utilized for bioimaging, biosensors, cancer diagnosis, and drug delivery, and so on.[6] Among them, propeller-shaped hexaphenylsilole (HPS) and tetraphenylethene (TPE) are archetypal AIE units. Currently, boron ketoiminate derivatives have also been found as AIE-active molecules. In 2008, James R. Gardinier's group first reported a series of β-ketoiminate complexes of difluoroboron, which are all green-blue emissive in the solid state but only very weakly emissive in fluid solution at room temperature.[7] Similarly, Yoshiki Chujo have also demonstrated that boron ketoiminate derivatives as a new class of highly emissive AIE fluorophores (in THF: Φ_{PL} = 0.01; in the solid state: Φ_{PL} = 0.30–0.76). Furthermore, the optical properties can be affected by the steric hindrance of the substituted groups on the nitrogen atom.[8a] However, the subsequent boron ketoiminate-based conjugated polymers developed by Yoshiki Chujo's group exhibited strong emission both in the solution and solid states ($\Phi_{PL,THF}$ = 0.46–0.80, $\Phi_{PL,film}$ = 0.13–0.38).[8b] That is, these polymers didn't show AIE behaviors. Recently, we have also synthesized some chiral β-ketoiminate-based polymers with similar structure, unfortunately, they are still not AIE-active.[4d] According to Tang's report, AIE-active molecules can undergo dynamic intramolecular rotations in dilute solution, but intramolecular rotations may be greatly

---

[a] Key Lab of Mesoscopic Chemistry of MOE, School of Chemistry and Chemical Engineering, Nanjing University, Nanjing 210093, China. E-mail: yxcheng@nju.edu.cn.
[b] Key Laboratory for Organic Electronics and Information Displays and Institute of Advanced Materials, Nanjing University of Posts and Telecommunications, Nanjing 210023, China. E-mail: iamlhwang@njupt.edu.cn.

† Electronic supplementary information (ESI) available: experimental details, NMR spectra of important compounds and particle size characterization of CPNs.

restricted owing to the physical constraint in the aggregate state. We think that these boron ketoiminate-based conjugated polymers cannot show AIE characteristics because they are lack of the rotatable plane within the polymer chain backbone. Based on this hypothesis, the AIE features of boron ketoiminate-based conjugated polymers can be realized and tuned by introducing rotatable plane in the well-designed polymer backbone, which can lead to strong fluorescence emission in aqueous media for bioprobes or bioimaging.

Conjugated polymer nanoparticles (CPNs) are an important class of nanoscale materials that possess prominent luminescent features for bioimaging, drug delivery, and tumour therapy due to high quantum yields, excellent photostability, and tunable multicolor emissions, low cytotoxicity.[9] AIE-active conjugated polymers can form nanoaggregates and exhibit strong fluorescence in the aqueous solution, which is desirable for biological application. Therefore, AIE-active conjugated polymers are inherently suitable for developing CPNs as bioprobes. Great effort should be focused on the improvement of yields and prolongation of emission wavelength. Herein, we designed and synthesized a series of AIE (AIEE)-active polymers by the conjugation of boron ketoiminate unit incorporating the rotatable phenyl ring on the nitrogen atom as shown in Scheme 1. Fluorene moiety was selected as a polymer linker because of their combined desirable properties, such as high charge-carrier-transporting ability, photostabilities, large molar absorptivities, and ease of syntheses.[10] Interestingly, the obtained boron ketoiminate-based polymers can exhibit obvious AIE (AIEE) behaviors in THF/water mixtures, and their emission wavelengths can be conveniently tuned by modulating the substituents in the phenyl ring on the nitrogen atom. In addition, CPNs from **P1**-**P4** could be prepared by reprecipitation as bioprobes for HeLa cell imaging.

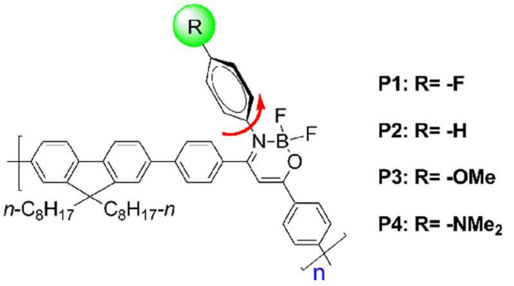

Scheme 1 Chemical structure of the conjugated polymers.

Results and discussion

Synthesis and characterization of the monomers and conjugated polymers

The detailed synthetic procedures of the monomers and conjugated polymers are illustrated in the supporting information (ESI 2). The chemical structures of the monomers **M1**-**M5** and the conjugated polymers **P1**-**P4** were characterized by ^{1}H NMR, ^{13}C NMR and ^{19}F NMR (ESI 8 in the supporting information). 2,7-dibromo-9,9-dioctyl-9*H*-fluorene **2** was synthesized in 81% yield through the alkylation reaction of 2,7-dibromo-9*H*-fluorene (**1**) and 1-bromooctane with potassium *t*-butoxide as base in DMF at 40 °C for 35 min. A Suzuki-Miyaura reaction between **2** and bis(pinacolato)diboron was performed in the presence of potassium acetate and Pd(dppf)Cl$_2$ in anhydrous DMSO at 65 °C for 15 h to afford 2,2'-(9,9-dioctyl-9*H*-fluorene-2,7-diyl)bis(4,4,5,5-tetramethyl-1,3,2-dioxaborolane) (**M1**) in 62% yield. The monomer **M2** was obtained by three reaction steps. A Michael addition reaction between 1-(4-bromophenyl)ethanone (**3**) and methyl 4-bromobenzoate (**4**) yielded (*Z*)-1,3-bis(4-bromophenyl)-3-hydroxyprop-2-en-1-one (**5**) as a light yellow crystal (75% yield). A condensation reaction between **5** and 4-fluoroaniline using *p*-toluenesulfonic acid as catalyst in a Dean–Stark apparatus for 36 h to afford (1*Z*,3*Z*)-1,3-bis(4-bromophenyl)-3-((4-fluorophenyl)imino)prop-1-en-1-ol (**6**) (28% yield). **7**, **8**, **9** were prepared by the same procedures with anilines containing the corresponding substituents in 32%, 35%, 37% yields, respectively. The boron ketoiminates **M2**-**M5** were prepared from the compounds **6-9** by the boron-complexation using BF$_3$·OEt$_2$ in high yields (above 90%). Finally, **P1**, **P2**, **P3** and **P4** were synthesized by the palladium-catalyzed Suzuki coupling reaction between **M1** and **M2**, **M3**, **M4**, **M5**, respectively. All the obtained conjugated polymers showed good solubility in nonpolar organic solvents, such as THF, *o*-xylene, toluene, chloroform, and dichloromethane, which can be attributed to the flexible alkyl side chain on the fluorene unit.

Optical properties of conjugated polymers

The optical properties of **P1**-**P4** in THF solution and aggregate states (10 μM) were carried out through UV-vis absorption and fluorescence (FL) spectra, and the relevant data are summarized in Table 1. **P1**, **P2**, **P3** and **P4** in THF solution exhibit two bands in the absorption spectra (Figure 1). **P1**-**P3** show similar absorptions, one band locates at around 300 nm, and the other band is situated at around 410 nm. Notably, **P4** in THF solution exhibits an obvious shoulder peak at around 292 nm and the other peak appears at 402 nm, which may be related to donor-acceptor interaction between dimethylamino unit and the boron-chealting ring.[3h]

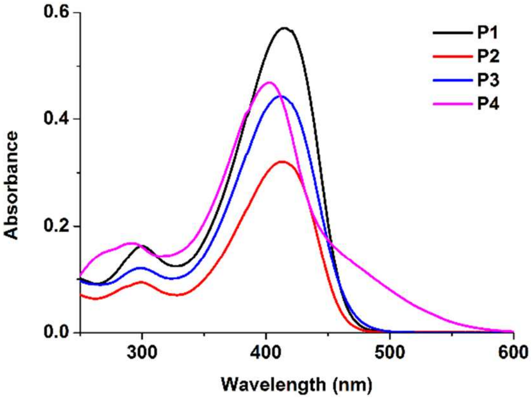

Fig. 1 UV/vis absorption spectra of **P1**-**P4** in THF solution (10 μM).

In this paper, the AIE (AIEE) characteristics can be investigated by adding different amounts of deionized water to the pure THF solutions of **P1**-**P4**, and the extent of aggregation can be adjusted by changing the water fractions (f_w) from 0 to 100%. The fluorescence spectra of **P1**-**P4** aggregates were performed when excited at 405 nm. As is evident from Figure 2, Both **P1** and **P2** show weak fluorescence emission in THF solutions, but the emission can exhibit enhancement response of different degrees when the water fraction (f_w) varies from 0% to 100%. From the pure THF solution to a mixture solution with f_w = 90%, the fluorescence intensities increases can reach as 14 and 12 folds for **P1** and **P2**, respectively, which demonstrates that **P1** and **P2** are AIEE-active. **P3** and **P4** are also very faintly fluorescent in THF solutions. And the fluorescence intensities have no obvious

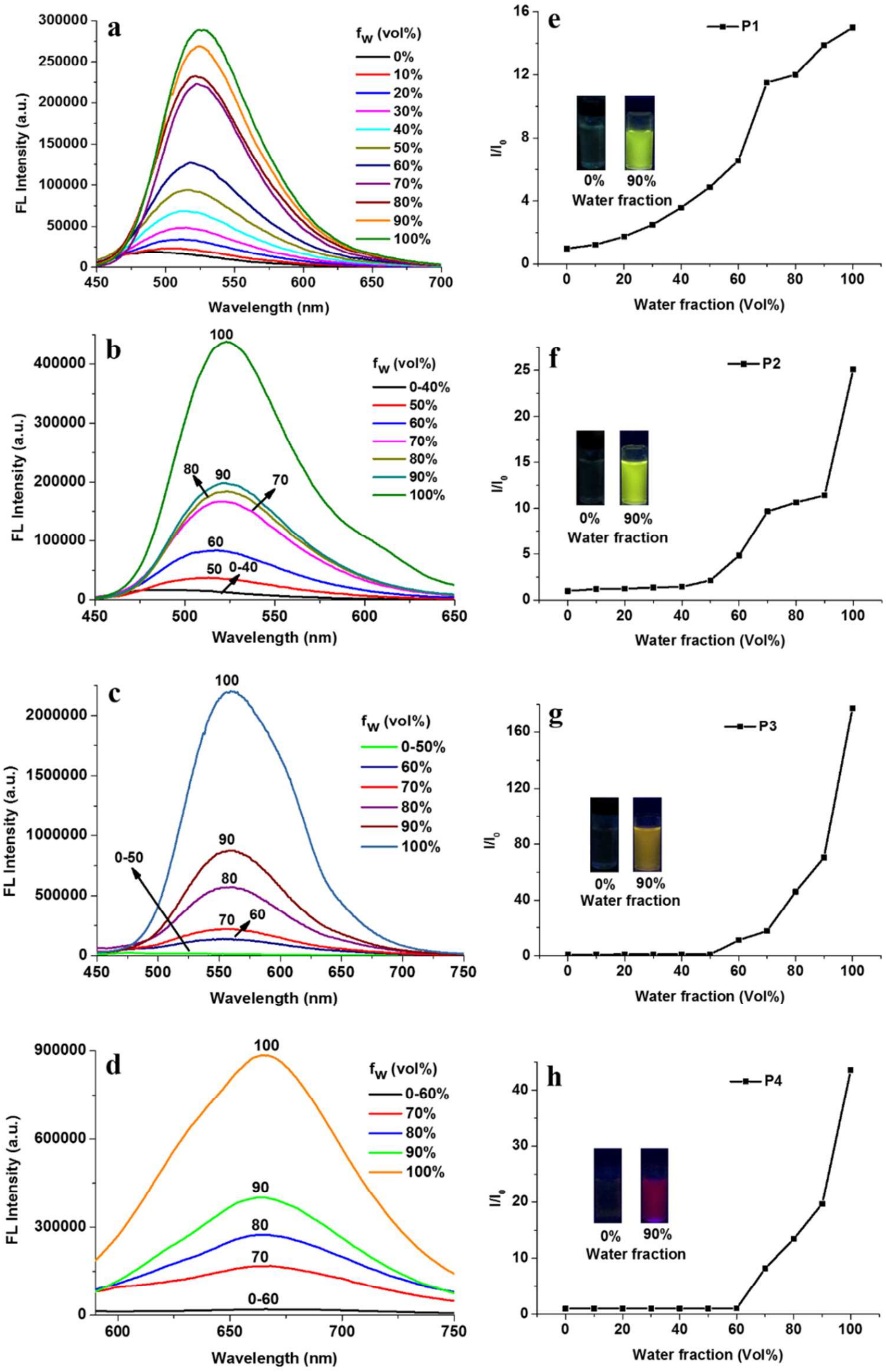

Fig. 2 Fluorescence spectra of (a) **P1**, (b) **P2**, (c) **P3**, and (d) **P4** in THF/water mixtures with different water fractions and Plot of I/I_0 of (e) **P1**, (f) **P2**, (g) **P3**, and (h) **P4** in THF/water mixtures, where I_0 and I are the emission intensity in pure THF solution and THF/water mixture, respectively. Inset shows photographs of solutions of **P1**-**P4** in THF and THF/ water mixtures (f_w = 90%) taken under UV illumination. The concentration of all solutions and suspensions is 10 μM, excited at 405.0 nm. The CPNs suspensions (f_w = 100%) were prepared by reprecipitaion (ESI 3 in the supporting information).

changes when $f_w < 60\%$. However, when f_w is 70% or higher, the intensities increase significantly with more addition of water, the fluorescence increases are 70 folds for **P3** and 20 folds for **P4** at $f_w = 90\%$, suggesting that **P3** and **P4** are AIE-active. Interestingly, compared to **P1**-**P3** in THF solution, that of **P4** shows a large Stokes shift (up to 253 nm), which can be ascribed to the strong interaction between dimethylamino substituted phenyl ring and the boron chelating ring. Furthermore, compared with **P1**-**P4** in THF solution, the emission wavelengths of **P1**-**P4** NPs show red shifts of 36, 41, 80 and 3 nm, respectively. The fluorescence quantum yields (Φ_{PL}) of **P1**-**P4** NPs are also increased to 0.31, 0.39, 0.15 and 0.07, respectively. Herein, **P4** NPs supension shows weaker fluorescence emission and less red shift than that of **P1**-**P3**, which is related to self-absorption from NIR by introducing N,N-dimethylbenzene amine on the nitrogen atom of boron ketoiminate moiety. Moreover, the quantum yield of **P4** NPs suspension can also be affected by polar microenvironments due to the existence of strong intramolecular donor-acceptor interaction.[11] Most importantly, the emission colors of CPNs can be tuned from green to red by linking different substituents on boron ketoiminate moiety, which derived from different electron-donating ability in the phenyl ring on the nitrogen in the polymer backbone. In order to better understand emission dynamics of CPNs and the fluorescence decay process, the fluorescence lifetimes for all the nanoparticles suspensions were investigated by time resolved technique and measured with the lifetime spectrometer FLS 920 under air. As shown in Figure 3, the analysis of the data by single exponential curves shows that fluorescence emission lifetime of CPNs are 1.17 ns for **P1**, 1.29 ns for **P2**, 1.15 ns for **P3** and 1.12 ns for **P4**, respectively, with the mean square deviation χ^2 (CHISQ) values ranging from 1.082 and 1.166 (Figure S18 in the supporting information).

Table 1 Summary data of optical properties of **P1-P4**

	In THF(1×10^{-5} mol/L) [a]			CPNs [a]	
	λ_{abs} (nm)	λ_{PL} (nm)	Φ [b]	λ_{PL} (nm)	Φ [b]
P1	300, 415	487	<0.01	523	0.31
P2	300, 413	480	<0.01	521	0.39
P3	298, 412	482	<0.01	562	0.15
P4	292, 403	658	<0.01	661	0.07

[a] Excited at 405 nm. [b] Quantum yields were determined with Coumarine 153 in ethanol ($\Phi = 0.38$) as the fluorescence reference.

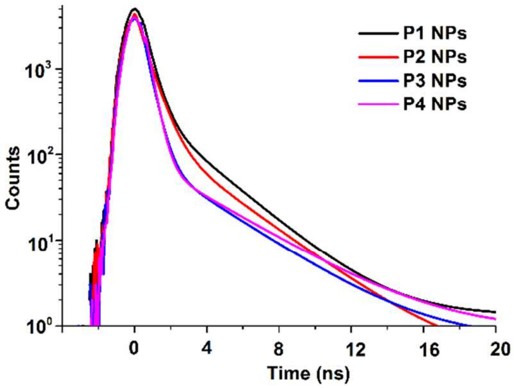

Fig. 3 Fluorescence decay curves of **P1-P4** NPs suspension (10 μM) All fluorescence lifetime measurements were obtained at an excitation from a laser tuned to $\lambda_{ex} = 405$ nm.

Preparation and characterization of CPNs

Aqueous dispersions of **P1-P4** NPs were prepared by using reprecipitation method as described in the reported work.[12] A THF solution containing conjugated polymer was quickly poured into water under sonication. A CPNs suspension was obtained after removal of THF and part of Milli-Q water under reduced pressure. The morphology and size of CPNs were analyzed by scanning electron microscopy (SEM) and dynamic light scattering (DLS). The particle size obtained from DLS indicates that the average hydrodynamic diameters of **P1-P4** NPs are 104.5 nm, 96.1 nm, 86.9 nm and 97.5 nm, respectively (Figure S17 in the supporting information). Meanwhile, the SEM images shows that **P1-P4** can form spherical nanoparticles with an average size of ~ 95 nm, ~ 86 nm, ~ 75 nm, and ~ 85 nm, respectively (Figure S17 in the supporting information). The smaller size relative to the results measured by DLS is ascribed to CPNs shrinkage in dry state. CPNs can exhibit multicolor fluorescence spanning from green to red as shown in Figure 2e-2h under a commercially available UV lamp irradiation (365 nm), which can be clearly observed by the naked eye.

Theoretical calculations

To well understand the electronic features at the 4-positions of phenyl ring on the nitrogen atom of four boron ketoiminate-based conjugated polymers, we further performed density functional theory (DFT) calculation on the simplified model compounds constituting the corresponding repeat units. Model compounds are shown in Figure 4, all the alkyl chains in the polymer systems were replaced by methyl groups to reduce the calculation time. All the calculations were carried out with the Gaussian 09 program suite, and HOMO and LUMO energy levels were estimated from the optimized geometry by using the B3LYP functional and 6-31 G* basis set.[13] As shown in Figure 5, the LUMOs of the model compounds are mainly centered on the boron ketoiminate core, which is as an acceptor in the polymer backbone. When no electron donor appears (R=F and H), the HOMOs are mainly located on fluorene unit. If the substituent is relatively strong electron donor (R=MeO), the HOMOs are also spread over the substituted phenyl ring. Interestingly, dimethylamino group was chosen as the strongest electron donor substituent, the HOMO is distributed only on the amino-substituted phenyl ring and boron chelating ring and the HOMO energy level is up to -4.99 eV. The calculated band gaps of Model 1 (R=F), Model 2 (R=H), Model 3 (R=MeO), and Model 4 ($R=NMe_2$) are 3.33, 3.40, 3.32, and 2.72 eV, respectively. The band gaps of Model 1 and Model 3 are very close and smaller than those of Model 2, but the band gap of Model 4 is the smallest. The results indicate that electronic structures of the conjugated polymers **P1-P4** can be affected by the substituents with different electron-donating ability, which can effectively tune their optical properties, especially on the color emission of these conjugated polymers.

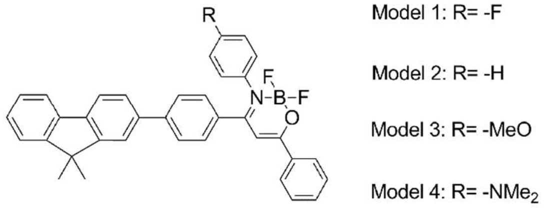

Fig. 4 Optimized model compounds from **P1-P4** for DFT calculations.

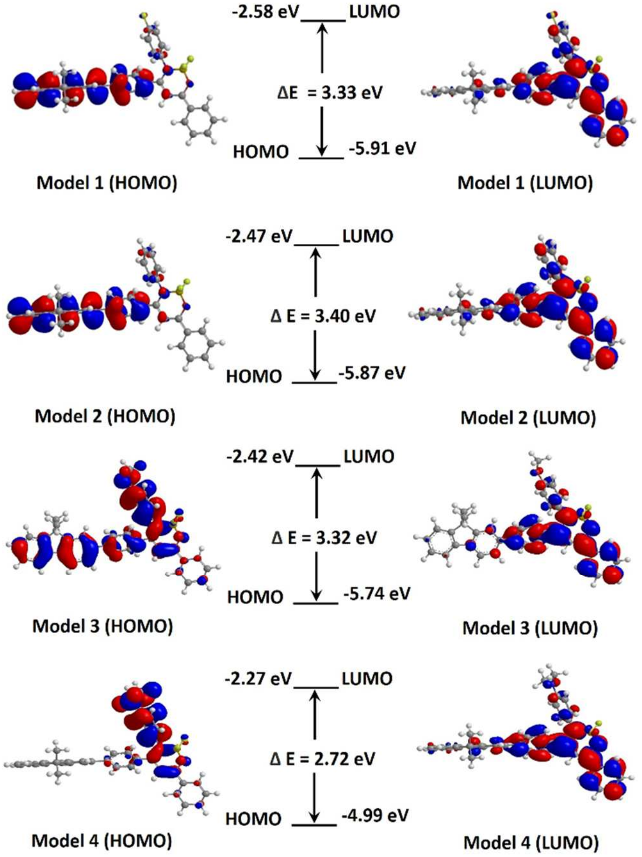

Fig. 5 Molecular orbital diagrams for the LUMOs and HOMOs of Model 1-4 from DFT calculations.

Cytotoxicity and photostability

As low toxicity is essential for biological applications, the cytotoxicity of **P1**-**P4** NPs against HeLa cells was estimated by MTT assays. Figure 6a-d shows the cell viability after incubation of **P1**-**P4** NPs at concentrations of 0, 5, 10, 20, and 40 μM for 48 h. The cell viabilities of these CPNs are close to 100% even at a high concentration of 40 μM within 48 h, which is indicative of the low cytotoxicity of **P**1-**P4** NPs suspension. In addition, the excellent photostability of fluorescent probes in aqueous media is also of great importance, especially for long-term imaging studies. The photostability of **P1**-**P4** NPs in HeLa cells was investigated by monitoring their fluorescence changes upon incubation with PBS buffer solution at 37 °C for 0-10 minutes, which was examined by CLSM under continuous laser scanning upon excitation at 405 nm (5 mW). As shown in Figure 6e, after 10 min continuous laser scanning, fluorescence intensity loss of the **P1**, **P2**, **P3** and **P4** NPs are only ~ 14%, ~ 12%, ~ 15%, and ~ 17%, respectively, indicating these CPNs have good photostability with an excellent resistance to laser irradiation. These results demonstrate that these boron ketoiminate-based conjugated polymer NPs are promising materials for live cell imaging.

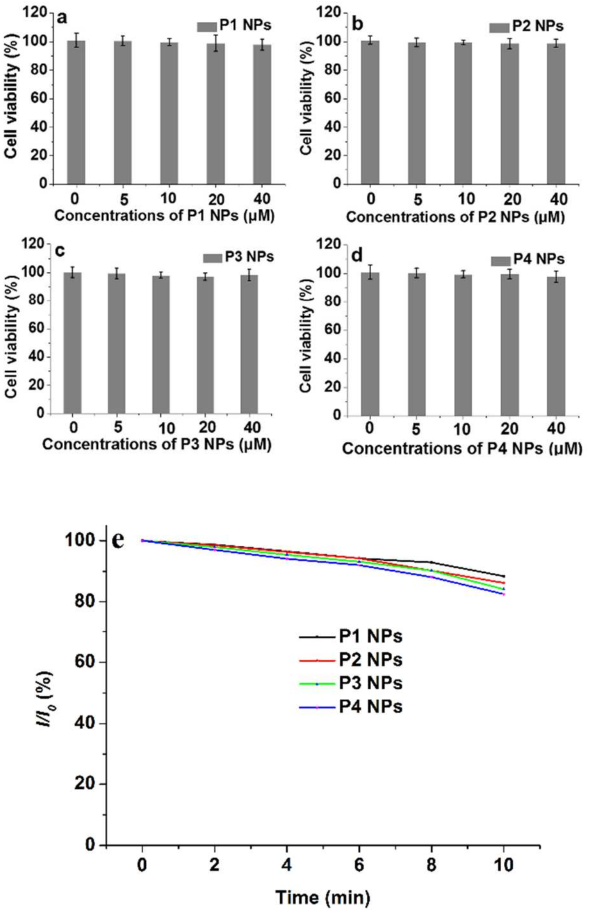

Fig. 6 (a-d) Metabolic viability of HeLa cells after incubation with **P1**-**P4** NPs suspension at different concentrations for 48 h. (e) Photostability of **P1**-**P4** NPs upon continuous laser excitation at 405 nm with a laser power of 5 mW for 0–10 min. I_0 is the initial fluorescence intensity and I is the fluorescence intensity of each sample at different time intervals after continuous laser sacnning.

Cell imaging application of CPNs

In order to further explore the applicability of **P1**-**P4** NPs as fluorescence bioprobes, we used CPNs for *in vitro* HeLa cells imaging. Fluorescence imaging was investigated by a confocal laser scanning microscope (CLSM). Figure 7a-d shows the CLSM images of HeLa cells upon incubation with **P1**-**P4** NPs (3 μM) for 2 h at 37 °C in culture medium. The cells were subsequently imaged by CLSM with 405 nm laser excitation, and the fluorescence signals were collected at 500–600 nm for **P1**-**P3** and 600–700 nm for **P4**. As shown in Figure 7a and 7b, **P1** and **P2** NPs are mainly distributed as intense green fluorescence dots in the cell cytoplasm without serious aggregation. Figure 7c and 7d reveals a yellow fluorescence from **P3** NPs and red fluorescence from **P4** NPs with similar distribution of **P1** NPs in the cytoplasm, and some nanoparticles can enter cellular nuclei, which is possibly due to their smaller sizes. These results also indicated an efficient intracellular uptake of the formulated NPs.

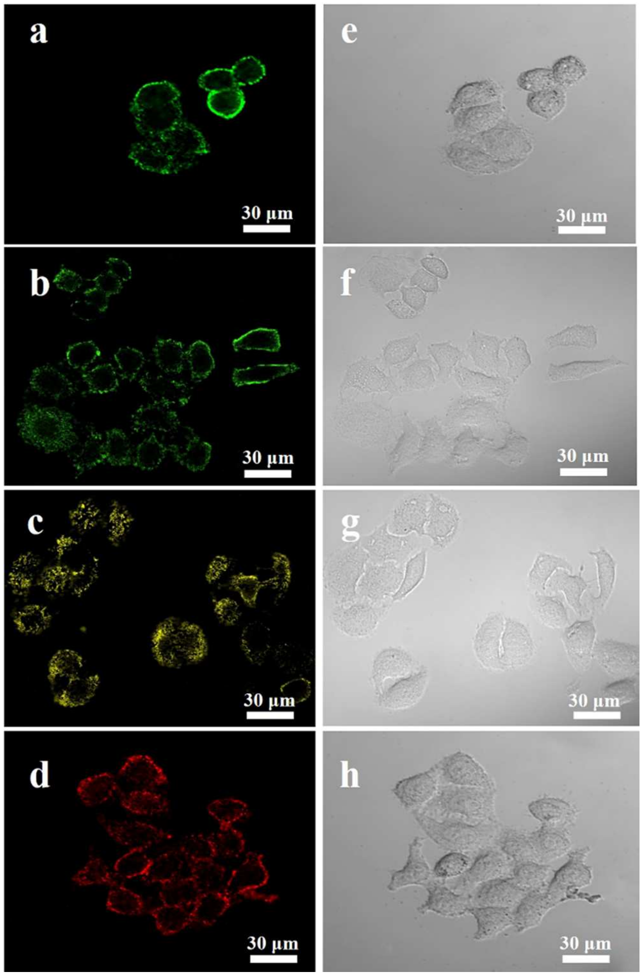

Fig. 7 Confocal laser scanning microscopy (CLSM) images of the HeLa stained with (a) **P1**, (b) **P2**, (c) **P3**, and (d) **P4** NPs. Bright-field images (e-h). The fluorescence was recorded under 405 nm excitation wavelength.

Conclusions

In summary, four boron ketoiminate-based conjugated polymers can exhibit typical AIE (AIEE) feature, and their tunable color of nanoparticles suspension can be successfully realized by the substituents with different electron-donating abilities. Furthermore, these polymers NPs can exhibit good photostability, low cytotoxicity with an average diameter of ~ 85–95 nm, which can be successfully utilized as fluorescence probes for HeLa for cell imaging.

Acknowledgements

This work was supported by the National Natural Science Foundation of China (21174061, 51173078, 21172106, and 21474048) and open project of Beijing National Laboratory for Molecular Sciences.

Notes and references

1 (a) Q. G. Wu, M. Esteghamatian, N. X. Hu, Z. Popovic, G. Enright, S. R. Breeze, and S. N. Wang, *Angew. Chem. Int. Ed.*, 1999, **38**, 985; (b) D. Mutaguchi, K. Okumoto, Y. Ohsedo, *Org. Electron.*, 2003, **4**, 49; (c) H. Kobayashi, N. Sato, Y. Ichikawa, M. Miyata, Y. Chujo, T. Matsuyama, *Synth. Met.*, 2003, **135-136**, 393; (d) X. Y. Wang and M. Weck, *Macromolecules*, 2005, **38**, 7219; (e) N. Sato, H. Ogawa, F. Matsumoto, Y. Chujo, T. Matsuyama, *Synth. Met.*, 2005, **154**, 113; (f) H. Kim, Y. J. Kang, E. S. Jeong, S. Kang, and K. T. Kim, *ACS Macro Lett.*, 2012, **1**, 1194; (g) Y. Kajiwara, A. Nagai, K. Tanakaa and Y. Chujo, *J. Mater. Chem. C*, 2013, **1**, 4437; (h) L. Wang, K. Wang, B. Zou, K. Q. Ye, H. Y. Zhang, and Y. Wang, *Adv. Mater.*, 2015, **27**, 2918; (i) C. D. Dou, Z. C. Ding, Z. J. Zhang, Z. Y. Xie, J. Liu, and L. X. Wang, *Angew. Chem. Int. Ed.*, 2015, **54**, 3648; (j) L. Wang, K. Wang, H. Y. Zhang, C. J. Jiao, B. Zou, K. Q. Ye, H. Y. Zhang and Y. Wang, *Chem. Commun.*, 2015, **51**, 7701.

2 (a) K. Tanaka , Y. Chujo, *Macromol. Rapid Commun.*, 2012, **33**, 1235; (b) N. Matsumi, Y. Chujo, *Polym. J.*, 2008, **40**, 77; (c) A. Nagai and Y. Chujo, *Chem. Lett.*, 2010, **39**, 430; (d) F. Jäkle, *Chem. Rev.*, 2010, **110**, 3985.

3 (a) N. Matsumi, K. Kotera, and Y. Chujo, *Macromolecules*, 2000, **33**, 2801; (b) F. Matsumoto and Y. Chujo, *Macromolecules*, 2003, **36**, 5516; (c) Y. Qin, C. Pagba, P. Piotrowiak, and F. Jäkle, *J. Am. Chem. Soc.*, 2004, **126**, 7015; (d) A. Nagai, K. Kokado, Y. Nagata, and Y. Chujo, *Macromolecules*, 2008, **41**, 8295; (e) A. Nagai, J. Miyake, K. Kokado, Y. Nagata, and Y. Chujo, *J. Am. Chem. Soc.*, 2008, **130**, 15276; (f) Y. Tokoro, A. Nagai, K. Kokado, and Y. Chujo, *Macromolecules*, 2009, **42**, 2988; (g) S. Cataldo, S. Fabiano, F. Ferrante, F. Previti, S. Patanè, B. Pignataro, *Macromol. Rapid Commun.*, 2010, **31**, 1281; (h) R. Yoshii, A. Hirose, K. Tanaka, and Y. Chujo, *J. Am. Chem. Soc.*, 2014, **136**, 18131.

4 (a) Y. Z. Wu, X. R. Mao, X. Ma, X. B. Huang, Y. X. Cheng, C. J. Zhu, *Macromol. Chem. Phys.*, 2012, **213,** 2238; (b) X. Ma, X. R. Mao, S. W. Zhang, X. B. Huang, Y. X. Cheng, and C. J. Zhu, *Polym. Chem.*, 2013, **4**, 520; (c) X. Ma, X. X. Jiang, S. W. Zhang, X. B. Huang, Y. X. Cheng, and C. J. Zhu, *Polym. Chem.*, 2013, **4**, 4396; (d) X. X. Jiang, X. H. Liu, Y. L. Jiang, Y. W. Quan, Y. X. Cheng, and C. J. Zhu, *Macromol. Chem. Phys.*, 2014, **215**, 358; (e) X. Ma, E. A. Azeem, X. L. Liu, Y. X. Cheng, and C. J. Zhu, *J. Mater. Chem. C*, 2014, **2**, 1076; (f) S. W. Zhang, Y. Sheng, G. Wei, Y. W. Quan, Y. X. Cheng, C. J. Zhu, *J. Polym. Sci., Part A: Polym. Chem.*, 2014, **52**, 1686.

5 (a) M. Wang, G. X. Zhang, D. Q. Zhang, D. B. Zhu, and B. Z. Tang, *J. Mater. Chem.*, 2010, **20**, 1858; (b) Y. N. Hong, J. W. Y. Lamab, and B. Z. Tang, *Chem. Soc. Rev.*, 2011, **40**, 5361; (c) D. Ding, K. Li, B. Liu, and B. Z. Tang, *Acc. Chem. Res.*, 2013, **46**, 2441; (d) J. Mei, Y. N. Hong, J. W. Y. Lam, A. J. Qin, Y. H. Tang, and B. Z. Tang, *Adv. Mater.*, 2014, **26**, 5429.

6 (a) R. R. Hu, N. L. C. Leungb, and B. Z. Tang, *Chem. Soc. Rev.*, 2014, **43**, 4494; (b) X. Q. Zhang, X. Y. Zhang, L. Tao, Z. G. Chi, J. R. Xu and Y. Wei, *J. Mater. Chem. B*, 2014, **2**, 4398; (c) G. G. Liu, D. D. Chen, L. W. Kong, J. B. Shi, B. Tong, J. G. Zhi, X. Feng and Y. P. Dong, *Chem. Commun.*, 2015, **51**, 8555.

7 F. P. Macedo, C. Gwengo, S. V. Lindeman, M. D. Smith, and J. R. Gardinier, *Eur. J. Inorg. Chem.*, 2008, 3200.

8 (a) R. Yoshii, A. Nagai, K. Tanaka, and Y. Chujo, *Chem. Eur. J.*, 2013, **19**, 4506; (b) R. Yoshii, A. Nagai, K. Tanaka, Y. Chujo, *Macromol. Rapid Commun*, 2014, **35**, 1315.

9 (a) X. L. Feng, F. T. Lv, L. B. Liu, H. W. Tang, C. F. Xing, Q. Yang and S. Wang, *ACS Appl. Mater. Interfaces*, 2010, **2**, 2429; (b) J. Pecher and S. Mecking, *Chem. Rev.*, 2010, **110**, 6260; (c) K. Li, and B. Liu, *J. Mater. Chem.*, 2012, **22**, 1257; (d) Y. Q. Li, J. Liu, B. Liu, and N. Tomczak, *Nanoscale*, 2012, **4**, 5694; (e) L. H. Feng, C. L. Zhu, H. X. Yuan, L. B. Liu, F. T. Lv and S. Wang, *Chem. Soc. Rev.*, 2013, **42**, 6620; (f) L. H. Feng, L. B. Liu, F. T. Lv, G. C. Bazan, and S. Wang, *Adv. Mater.*, 2014, **26**, 3926; (g) J. L. Geng, C. Y. Sun, J. Liu, L. D. Liao, Y. Y. Yuan, N. Thakor, J. Wang, and B. Liu, *small*, 2015, **11**, 1603.

10 (a) U. Scherf, D. Neher, Polyfluorenes; Springer: Berlin, 2008; Vol. 212; (b) P. Najechalski, Y. Morel, O. Stephan, P. L. Baldeck, *Chem. Phys. Lett.*, 2001, **343**, 44; (c) M. Leclerc, *J. Polym. Sci., Part A: Polym. Chem.*, 2001, **39**, 2867.

11 M. Pannipara, A. M. Asiri, K. A. Alamry, M. N. Arshad, S. A. El-Daly, *Spectrochim. Acta A*, 2015, **136**, 1893-1902.

12 B.Q. Bao, N. J. Tao, D. L. Yang, L. H. Yuwen, L. X. Weng, Q. L. Fan, W. Huang and L. H. Wang, *Chem. Commun.*, 2013, **49**, 10623.

13 M. J. Frisch, G. W. Trucks, H. B. Schlegel, G. E. Scuseria, M. A. Robb, J. R. Cheeseman, G. Scalmani, V. Barone, B. Mennucci, G. A. Petersson, H. Nakatsuji, M. Caricato, X. Li, H. P. Hratchian, A. F. Izmaylov, J. Bloino, G. Zheng, J. L. Sonnenberg, M. Hada, M. Ehara, K. Toyota, R. Fukuda, J. Hasegawa, M. Ishida, T. Nakajima,

Y. Honda, O. Kitao, H. Nakai, T. Vreven, J. A. Montgomery, Jr, J. E. Peralta, F. Ogliaro, M. Bearpark, J. J. Heyd, E. Brothers, K. N. Kudin, V. N. Staroverov, R. Kobayashi, J. Normand, K. Raghavachari, A. Rendell, J. C. Burant, S. S. Iyengar, J. Tomasi, M. Cossi, N. Rega, J. M. Millam, M. Klene, J. E. Knox, J. B. Cross, V. Bakken, C. Adamo, J. Jaramillo, R. Gomperts, R. E. Stratmann, O. Yazyev, A. J. Austin, R. Cammi, C. Pomelli, J. W. Ochterski, R. L. Martin, K. Morokuma, V. G. Zakrzewski, G. A. Voth, P. Salvador, J. J. Dannenberg, S. Dapprich, A. D. Daniels, Ö. Farkas, J. B. Foresman, J. V. Ortiz, J. Cioslowski and D. J. Fox, Gaussian 09, Revision A.2, Gaussian, Inc., Wallingford CT, 2009

Graphic Abstract